

10th Eco-Energy and Materials Science and Engineering
(EMSES2012)

Effect of Annealing Temperature on the Photocatalytic Activity of TiO₂ Thin Films

C.-P. Lin, H. Chen, A. Nakaruk, P. Koshy, C.C. Sorrell*

School of Materials Science and Engineering, University of New South Wales, Sydney, NSW 2052, Australia

Abstract

TiO₂ thin films were spin coated on soda-lime-silica glass substrates under identical conditions and then annealed for 2 h in air in the range of 300°-500°C in increments of 50°C. The mineralogical, morphological, optical, and photocatalytic properties then were assessed for the films. The techniques used were glancing-angle X-ray diffraction (GAXRD), field emission gun transmission electron microscopy (FEGTEM), field emission scanning electron microscopy (FESEM), atomic force microscopy (AFM), UV-VIS spectrophotometry (UV-VIS), and methylene blue (MB) degradation. The films had a consistent thickness of ~255 nm. Anatase peaks recrystallised at the annealing temperature of 400°C, with the crystallinity increasing with increasing annealing temperatures. Although recrystallisation caused a significant increase in grain size, the crystalline films showed only a slight increase in the grain size with increasing annealing temperatures. In contrast, the surface roughness of all of the films increased significantly with increasing annealing temperatures. This was associated with increased grain faceting, which was supported by the X-ray diffraction data.

All of the films showed high transparency in the visible region, with the optical indirect band gap of the crystalline films decreasing slightly from 3.49 eV to 3.43 eV with increasing annealing temperatures. Four regimes of photocatalytic performance could be identified, which depended principally on the degree of crystallinity and the level of contamination. In short, a blank was used to negate heating effects, the amorphous films were inert, the onset of crystallisation established photoactivity, and the photoactivity of the films annealed at 400°-500°C decreased in a trend consistent with the trends in increasing grain size, increasing surface roughness, increasing crystallinity, decreasing band gap, and increasing contamination. Since this consistency was the case, these variables could not be decoupled. For the samples that were fabricated using the specified materials and methods, characterised, and tested, the optimal temperature for annealing was found to be 400°C.

© 2013 The Authors. Published by Elsevier B.V. Open access under [CC BY-NC-ND license](https://creativecommons.org/licenses/by-nc-nd/4.0/).

Selection and peer-review under responsibility of COE of Sustainable Energy System, Rajamangala University of Technology Thanyaburi (RMUTT)

Keywords: TiO₂; Thin Films; Spin Coating; Photocatalysis; Crystallinity

*C.C. Sorrell, Tel.: (+61-2) 9385-4421; fax: (+61-2) 9385-6565

E-mail address: c.sorrell@unsw.edu.au

1. Introduction

Over the last decade, extensive research has been conducted on investigating the photocatalytic properties of titanium dioxide (TiO₂, titania) for applications such as photovoltaic cells [1], water purification systems [2], and self-cleaning and self-sterilising materials [3]. For the abovementioned applications, thin films are more extensively used than bulk materials owing to cost considerations, processing flexibility, and suitability for various substrates, types and shapes.

Generally, the optical band gap (E_g) of TiO₂ varies with its structure, with the value for amorphous TiO₂ being ~3.5 eV [4] and the values for crystalline anatase and rutile being 3.2 eV and 3.0 eV [5], respectively. As rutile can absorb light of a wider wavelength range, it would be assumed that the photocatalytic performance of rutile would be superior to that of anatase. However, anatase provides higher photocatalytic activity owing to the higher density of localised states, consequent surface-adsorbed hydroxyl radicals, and slower charge carrier recombination rate relative to rutile [6,7]. As a result, there is growing interest in understanding the unique photocatalytic activity of anatase.

TiO₂ thin films can be synthesised using different techniques, including sputtering [8], laser ablation [9], electrophoretic deposition [10], anodic oxidation [11], sol-gel [12], screen printing [13], dip coating [14], gel oxidation [15], spray pyrolysis [16], and spin coating [17]. Spin coating is used widely in the fabrication of TiO₂ thin films due to rapid growth rates, capacity for handling large sample sizes, mass production capability, and high yield rates [18,19]. However, the spin coating technique involves a subsequent annealing process, which is known to enhance the diffusion of contaminants from the glass substrate to the coating [20,21]. This process tends to restrict the grain growth in the film and also increases the number of lattice defects, which decreases the photocatalytic activity of the TiO₂ thin films.

The intentions of the present work were to synthesise TiO₂ thin film coatings on glass substrates using spin coating and to determine the optimal annealing temperature, which should produce the best photocatalytic performance. This is an extension of previous work [17] that focused on the phase transformation of anatase → rutile. Further, the present work focussed on the effect of contamination from the substrate (viz., Na, Ca, and Si) on the film properties, including mineralogical, morphological, optical, and photocatalytic.

2. Methodology

The method used to fabricate the TiO₂ thin films by spin coating is described in detail elsewhere [21]. Briefly, the precursors used were titanium isopropoxide (TIP) dissolved in isopropanol at 0.1 M Ti concentration. The solutions were mixed in a Pyrex beaker by hand-stirring for 1 min without heating. Spin coating was done by rapidly depositing ~0.2 mL of solution onto a soda-lime-silica glass substrate that was spun at 2000 rpm in air. The film was dried by spinning for an additional 15 s and the overall process was repeated six more times. Subsequent annealing was carried out in a muffle resistance furnace at annealing temperatures that varied in the range 300°-500°C for times of 2 h; the heating rate used was 5°C/min, followed by natural cooling.

The thickness of the films was determined using field emission gun transmission electron microscopy (FEGTEM, 200 kV accelerating voltage, *Philips CM200*). The mineralogy of the films was examined using glancing-angle X-ray diffraction (GAXRD, 45 kV, 40 mA, *PAN-analytical X'pert Materials Research Diffractometer*). The grain size was estimated by field emission scanning electron microscopy

(FESEM, 3 kV accelerating voltage, *FEI Nova NanoSEM 230*). The surface roughness was determined using atomic force microscopy (AFM, tapping mode, *Bruker Dimension Icon SPM*). Film contamination was determined by X-ray photoelectron spectroscopy (XPS, 15.2 kV, 10.8 mA, *Thermo Scientific ESCALAB250Xi*). The optical properties of the films were analysed using UV-VIS spectrophotometry (UV-VIS, *PerkinElmer Lambda 35*).

The photocatalytic performance of the TiO₂ thin films was determined from the photobleaching of methylene blue (MB) solution upon exposure of the film/substrate to UV light (365 nm, 8 W, 10 cm sample-light distance) for 2 h. The MB solutions were prepared by dissolving methylene blue in deionised water at 10⁻⁵ M concentration [22] and stirring manually in a Pyrex beaker for 5 min without heating. The exposed MB solutions then were analysed using the UV-VIS spectrophotometer.

3. Results and Discussion

Figure 1 shows TEM images of the films annealed at 400°C and 500°C. Table 1 shows that the thickness of the films was relatively consistent at an average of ~255 nm. This result indicates that the annealing temperature had little effect on the film thickness. The nanostructural differences visible in the TEM images resulted from the partially amorphous (400°C) and crystalline (500°C) natures of the films, as discussed subsequently.

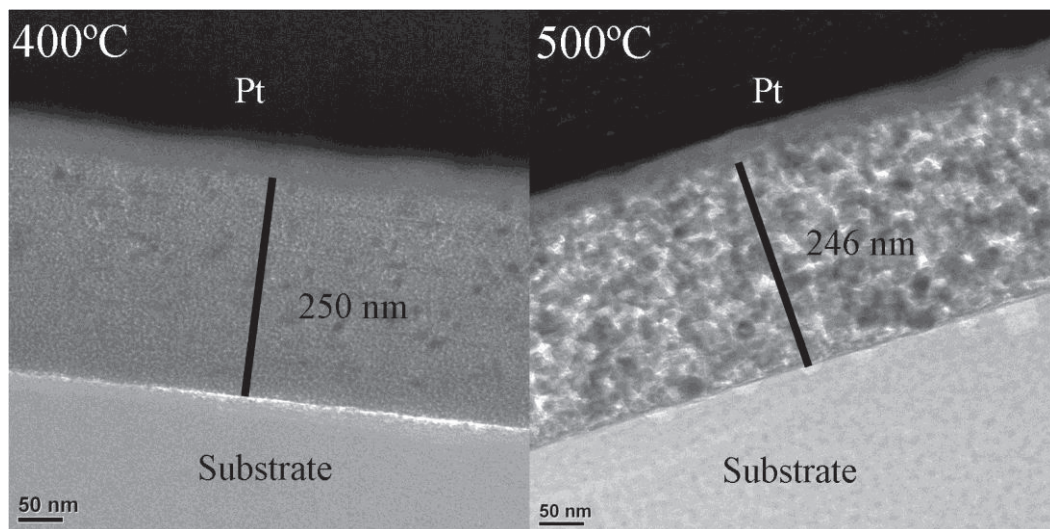
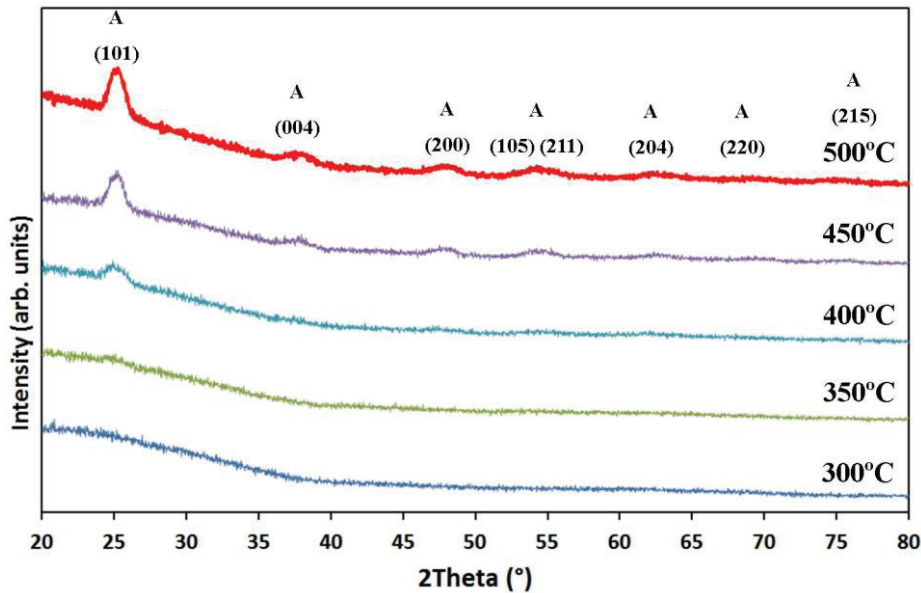


Fig. 1. TEM images of TiO₂ thin films annealed at different temperatures

Figure 2 shows the mineralogy of the films annealed at different temperatures for 2 h. From these data, it can be seen that, at 300°C and 350°C, the films were amorphous. The (101) anatase peak appeared at the annealing temperature of 400°C and the crystallinity further increased with increasing annealing temperature, as shown by the increased peak height. This is evident from the XRD pattern of the film heated at 500°C, which shows all of the major anatase peaks.

Table 1. Summary of analytical data

Parameters	Units	Annealing Temperature				
		300°C	350°C	400°C	450°C	500°C
Mineralogy	--	Amorphous	Amorphous	Anatase	Anatase	Anatase
Average Grain Size	nm	~10	~10	~23	~26	~29
Arithmetic Surface Roughness	nm	0.32	0.42	0.59	0.89	0.96
Film Thickness	nm	~260	~257	~250	~250	~246
Transmission in Visible Range	%	~80	~80	~80	~80	~80
Optical Indirect Band Gap	eV	3.49	3.49	3.49	3.45	3.43
Na Level	at%	1.38	1.46	2.07	4.24	5.73
Ca Level	at%	0	0	0	0.39	0.53
Si Level	at%	1.13	1.29	1.63	2.17	3.11
Na + Ca + Si Level	at%	2.51	2.75	3.70	6.80	9.37
Ti Level	at%	27.89	27.61	27.32	26.31	25.79
(Na + Ca + Si)/Ti Level	--	9.00	9.96	13.54	25.85	36.33

Fig. 2. GAXRD patterns of TiO₂ thin films annealed at different temperatures

While it is known that anatase can crystallise at 300°C [23], with thin films, the anatase → rutile transformation temperature also depends on the degree and/or type of contamination [17,21]. The glass substrate contains Na₂O, CaO, and SiO₂ as the major components, of which Na and Si are known to diffuse at high levels into the film at relatively modest annealing temperatures [20]. Further, Si is known to be a grain growth inhibitor and to increase the temperature required for recrystallisation of anatase [7]. The XPS data, discussed subsequently, confirm that the films contained Na and Si as the main

contaminants. Therefore, since diffusion is a temperature-dependent process, it is expected that the level of contamination would be a function of the annealing temperature.

The surface morphology of the films is shown in Figure 3. The AFM images and data, as shown in Table 1, indicate that the grain size increased significantly upon recrystallisation although, once this occurred, little subsequent growth with increasing annealing temperature took place. In contrast, the surface roughness appeared to increase monotonically with increasing annealing temperature. This indicates that little densification occurred (as confirmed by the low amount of grain growth) and that the grains became more euhedral (faceted) with increasing annealing temperature. This observation is supported by the GAXRD data, which showed that increasing annealing temperature resulted in enhanced crystallinity of the films.

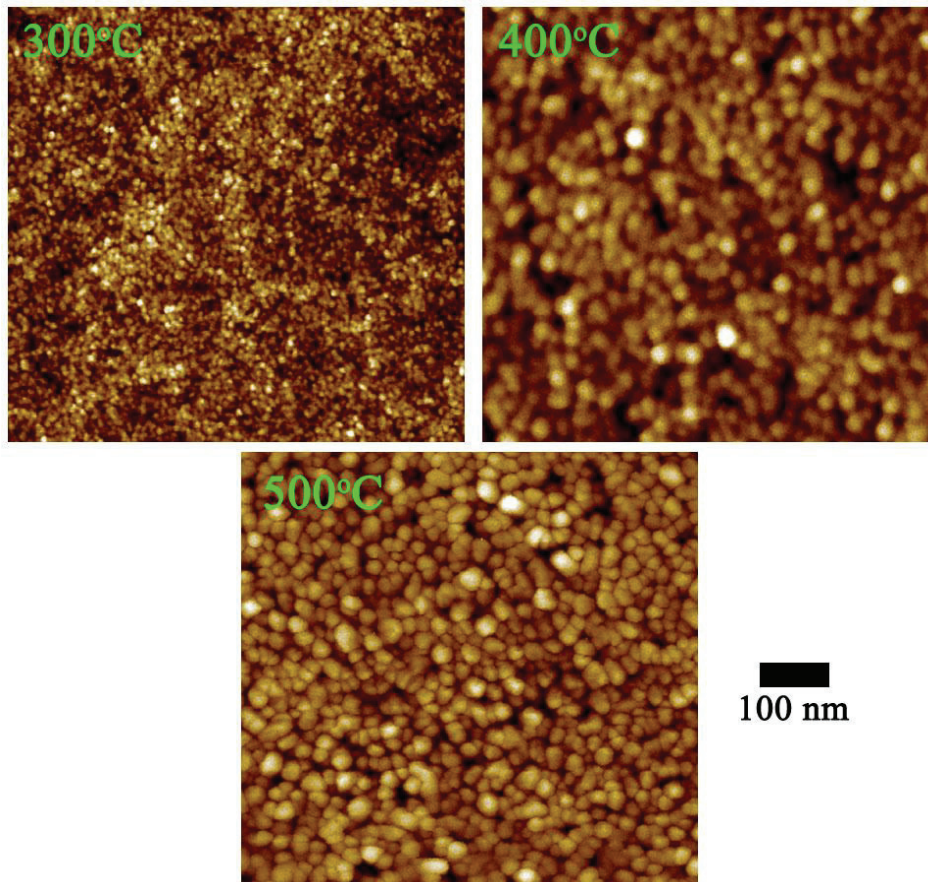


Fig. 3. AFM surface morphologies of TiO_2 thin films annealed at different temperatures

The optical transmission spectra of the films are shown in Figure 4, which shows that all of the films were highly transparent in the visible region. The data also show that the films were relatively flat, as indicated by the interference fringes. The optical indirect band gap was calculated using the method of Tauc and Menth [24]:

$$(\alpha h\nu)^{1/2} = C(h\nu - E_g) \quad (1)$$

Where: α = $-(1/d)\ln(T/100)$
 d = Film thickness (cm)
 T = Optical transmittance (%)
 h = Planck's constant (4.136×10^{-15} eV.s)
 ν = Frequency of light (s^{-1})
 C = Constant
 E_g = Optical indirect band gap (eV)

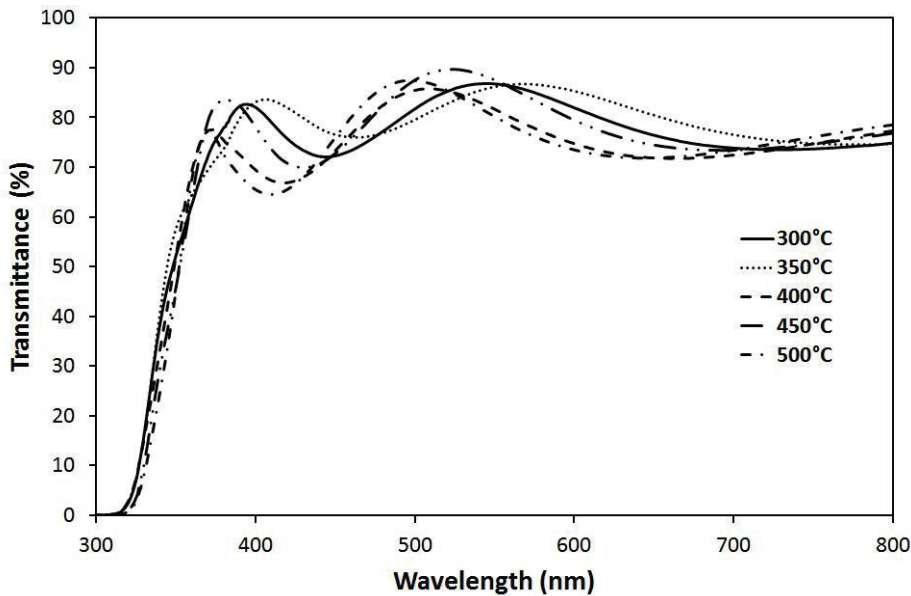


Fig. 4. UV-VIS optical transmission spectra of TiO₂ thin films annealed at different temperatures

The values of E_g , given in Table 1, were extrapolated from the absorption edge to the abscissa of the plot of $(\alpha h\nu)^{1/2}$ versus $h\nu$. The band gaps of the films slightly decreased with increasing annealing temperature probably owing to the increasing degree of crystallinity of the films and increasing level of contamination [20]. The data for the photodegradation of the MB solution following irradiation are shown in Figure 5. It can be seen from the curves, particularly the peak at ~ 665 nm, that the photocatalytic performance did not show a linear trend and that the best performance was for the film annealed at 400°C; this will be discussed subsequently.

Figure 6 shows the extent of (Na + Ca + Si)/Ti contamination of the films, as determined from the XPS analyses. These data show that contamination was minimal at the two lowest annealing temperatures and that the onset of contamination commenced at $\sim 400^\circ\text{C}$, thereafter increasing with higher annealing temperatures. Figure 7 plots the data at ~ 665 nm from Figure 5 in terms of the degree of photodegradation. The data for the two figures can be interpreted in terms of four regimes that can be identified:

- Regime I: Photodegradation from UV light only (no film/substrate)
- Regime II: No effect from TiO₂ since it is amorphous
- Regime III: Increase in photodegradation owing to recrystallisation of anatase
- Regime IV: Decreasing photodegradation owing to increasing cation contamination

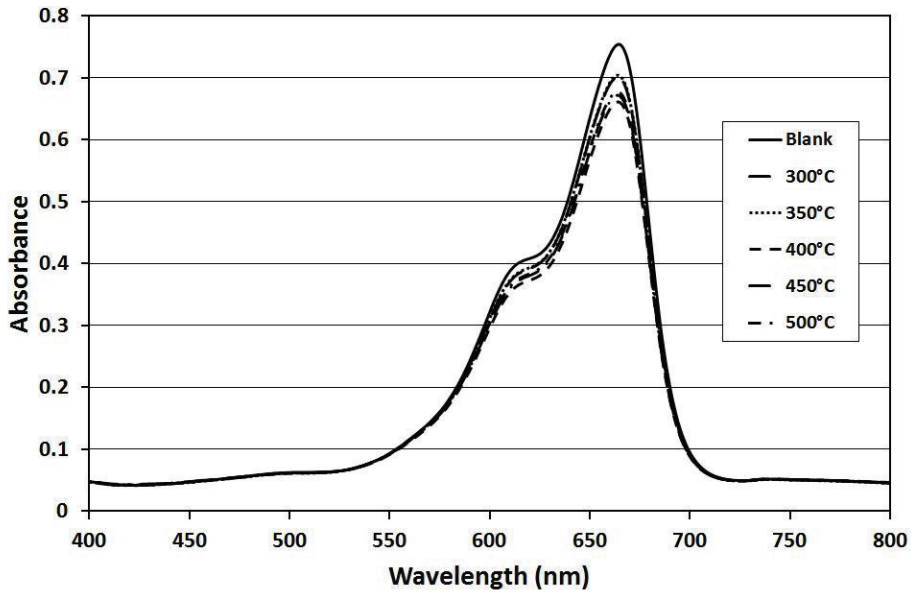


Fig.. 5. Photodegradation of MB solution by TiO₂ thin films annealed T different temperatures

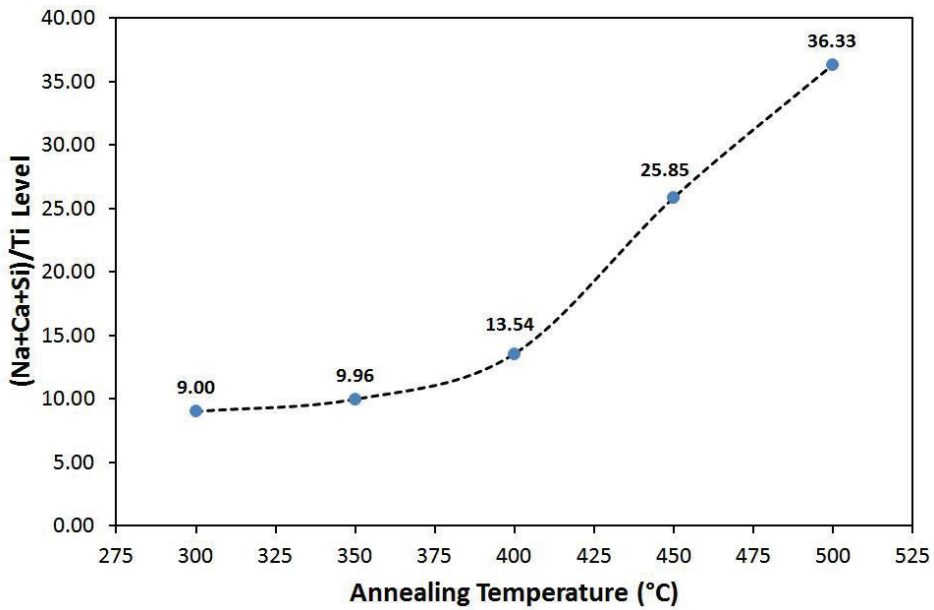


Fig. 6. Extent of (Si +Ca + Na)/Ticontamination in TiO₂ thin films annealed at different temperatures

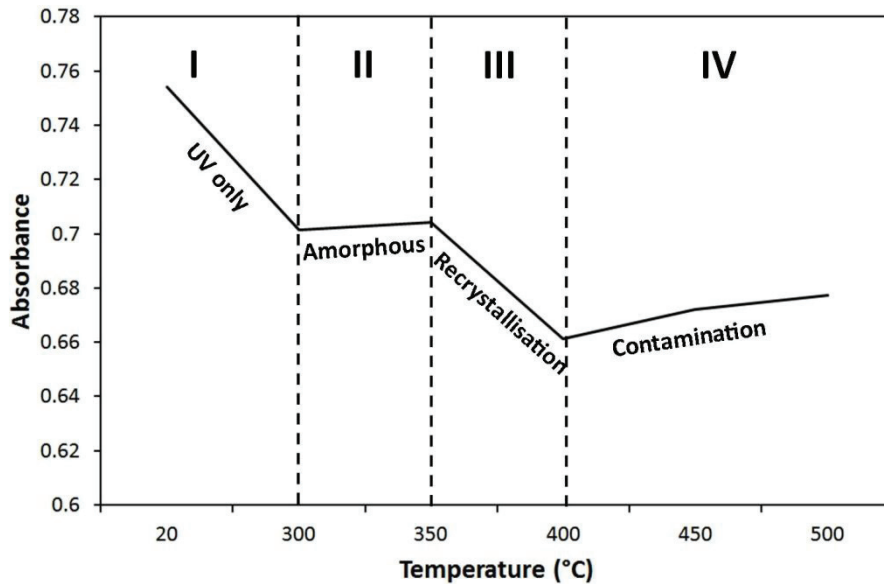


Fig. 7. Variation in absorbance with annealing temperature, highlighting the four regimes of photodegradation

Table 2 summarises the factors that affect the photocatalysis, photodegradation, and hence the nature of the four identified regimes. It is tempting to conclude from the data in Figure 6 that contamination is the main factor affecting performance since contaminant species are known to act as recombination sites for electrons and holes, thereby increasing the electron-hole recombination rates and reducing the photocatalytic performance [25,26]. However, Figure 7 clearly demonstrates that other factors, which are summarised in Table 2, also are relevant. Therefore, the effect of contamination cannot be decoupled from those of the grain size, surface roughness/area, crystallinity, and band gap.

Table 2. Factors affecting photocatalytic performance

Variable	Relevant Effect
Contamination	Electron and hole recombination sites as defects
Grain Size	Affects number of surface-active sites and hole diffusion distance
Surface Roughness/Area	Affects number of surface-active sites and recombination sites
Crystallinity	Affects light reflection and absorption
Band Gap/Absorption Edge	Amorphous → Crystalline = Inert → Photoactive
	Affects light absorption

4. Conclusions

In the present work, TiO₂ thin films deposited on soda-lime-silica glass substrates were prepared by spin coating, followed by annealing at temperatures of 300°C to 500°C for 2 h. GAXRD patterns showed that the films deposited at 300°C and 350°C were amorphous while those fabricated by annealing at higher temperatures consisted of anatase, with the proportion of crystalline phases increasing with increasing temperature. FESEM and AFM images indicated that, for the crystalline films, increasing annealing temperature resulted in slightly increasing grain size and significantly increasing surface

roughness while the film thickness remained at ~255 nm, regardless of the annealing temperature. While all of the films were highly transparent in the visible region (~80%), the optical indirect band gap decreased slightly with increasing annealing temperature.

The data for the photocatalytic activity of the films allowed identification of four regimes for photodegradation, corresponding largely to degrees of crystallinity and contamination. Examination of the data for grain size, surface roughness, crystallinity, band gap, and contamination indicates that, for the crystalline films, all of the trends are consistent. Consequently, it is not possible to decouple these effects.

For the total range of films, the photocatalytic performance showed an increase with increasing annealing temperature to 400°C, after which the performance was observed to decrease. One or more of the preceding variables is/are responsible for the decrease in the photocatalytic performance of the films at temperatures of 450°C and above. Thus, for an annealing time of 2 h, the optimal temperature for annealing TiO₂ thin films was determined to be 400°C.

Acknowledgements

This work was supported in part by a project funded by the Australian Research Council (ARC). The authors are grateful for the characterisation facilities provided by the Australian Microscopy & Microanalysis Research Facilities (AMMRF) node at the University of New South Wales (UNSW). H. Chen is thankful for the receipt of Postgraduate Research Support Scheme funding to present this work.

References

- [1] Chung I, Lee B, He J, Chang RPH, Kanatzidis MG. All-solid-state dye-sensitized solar cells with high efficiency. *Nature* 2012; **485**:486-89.
- [2] Nakata K, Fujishima A. TiO₂ photocatalysis: Design and applications. *J Photoch Photobio C* 2012; **13**:169-89.
- [3] Kamegawa T, Shimizu Y, Yamashita H. Superhydrophobic surfaces with photocatalytic self-cleaning properties by nanocomposite coating of TiO₂ and polytetrafluoroethylene. *Adv Mater* 2012; **24**:3697-700.
- [4] Fuyuki T, Matsunami H. Electronic properties of the interface between Si and TiO₂ deposited at very low temperatures. *Jpn J Appl Phys* 1986; **25**:1288-91.
- [5] Deng QR, Xia XH, Guo ML, Gao, Y, Shao G. Mn-doped TiO₂ nanopowders with remarkable visible light photocatalytic activity. *Mater Lett* 2011; **65**:2051-54.
- [6] Tayade RJ, Surolia PK, Kulkarni RG, Jasra RV. Photocatalytic degradation of dyes and organic contaminants in water using nanocrystalline anatase and rutile TiO₂. *Sci Technol Adv Mat* 2007; **8**:455-62.
- [7] Hanaor D, Sorrell CC. Review of the anatase to rutile phase transformation. *J Mater Sci* 2011; **46**:855-74.
- [8] Yasuda Y, Kamikuri K, Tobisaka M, Hoshi Y. Low-temperature deposition of crystallized TiO₂ thin films. *Thin Solid Films* 2012; **520**:3736-40.
- [9] Wang SJ, Chang WT, Ciou JY, Wei MK, Wong MS. Preparation of TiO₂ thin films by laser ablation for photocatalytic applications. *J Vac Sci Technol A* 2008; **26**:898-902.
- [10] Ghrairi N, Bouaicha M. Structural, morphological, and optical properties of TiO₂ thin films synthesized by the electro phoretic deposition technique. *Nanoscale Res Lett* 2012; **7**:1-17.
- [11] Zheng L, Cheng H, Liang F, Shu S, Tsang CK, Li H, et al. Porous TiO₂ photonic band gap materials by anodization. *J Phys Chem C* 2012; **116**:5509-15.
- [12] Tian J, Deng H, Sun L, Kong H, Yang P, Chu J. Effects of Co doping on structure and optical properties of TiO₂ thin films prepared by sol-gel method. *Thin Solid Films* 2012; **520**:5179-83.
- [13] Tsoukleris DS, Kontos AI, Aloupogiannis P, Falaras P. Photocatalytic properties of screen-printed titania. *Catal Today* 2007; **124**:110-7.

- [14] Behpour M, Atouf V. Study of the photocatalytic activity of nanocrystalline S, N-codoped TiO₂ thin films and powders under visible and sun light irradiation. *Appl Surf Sci*2012;**258**:6595-6601.
- [15] Puddu V, Choi H, Dionysiou DD, Puma GL. TiO₂ photocatalyst for indoor air remediation: Influence of crystallinity, crystal phase, and UV radiation intensity on trichloroethylene degradation. *Appl Catal B-Environ*2012;**95**:312-19.
- [16] Nakaruk A, Ragazzon D, Sorrell CC. Anatase–rutile transformation through high-temperature annealing of titania films produced by ultrasonic spray pyrolysis. *Thin Solid Films*2012;**518**:3735-42.
- [17] Nakaruk A, Lin CY, Perera DS, Sorrell CC. Effect of annealing temperature on titania thin films prepared by spin coating. *J Sol-Gel Sci Techn*2012;**55**:328-34.
- [18] Patil KR, Sathaye SD, Kholam YB, Deshpande SB, Pawaskar NR, Mandale AB. Preparation of TiO₂ thin films by modified spin-coating method using an aqueous precursor. *Mater Lett*2003;**57**:1775-80.
- [19] Suciu RC, Roşu MC, Silipaş TD, Biriş AR, Bratu I, Indrea E. TiO₂ thin films prepared by spin coating technique. *Rev Roum Chim*2011;**56**:607-12.
- [20] Yu J, Zhao X, Zhao Q. Photocatalytic activity of nanometer TiO₂ thin films prepared by the sol–gel method. *Mater Chem Phys*2001;**69**:25-9.
- [21] Nakaruk A, Lin CYW, Chaneei D, Koshy P, Sorrell CC. Fe-doped and Mn-doped titanium dioxide thin films. *J Sol-Gel Sci Techn*2012;**61**:175-8.
- [22] Mills A, McFarlane M. Current and possible future methods of assessing the activities of photocatalyst films. *Catal Today*2007;**129**:22-8.
- [23] Depero LE, Bonzi P, Zocchi M, Casale C, De Michele G. Study of the anatase-rutile transformation in TiO₂ powders obtained by laser-induced synthesis. *J Mater Res*1993;**8**:2709-15.
- [24] Tauc J, Mentha A. States in the gap. *J Non-Cryst Solids*1972;**8**:569-85.
- [25] Jones PM, Dunn S. Photo-reduction of silver salts on highly heterogeneous lead zirconate titanate. *Nanotechnology*2007;**18**:Article No. 185702.
- [26] Dong F, Guo S, Wang H, Li X, Wu Z. Enhancement of the visible light photocatalytic activity of C-doped TiO₂ nanomaterials prepared by a green synthetic approach. *J Phys Chem C*2011;**115**:13285-92.